2016 IEEE/RSJ International Conference on Intelligent Robots and Systems (IROS)
Daejeon Convention Center
October 9-14, 2016, Daejeon, Korea

Bipedal Walking Pattern Generation Based on an Extrapolated Center of Mass

Sangsin Park[1] and Jun-Ho Oh[1]

Abstract— **For a biped robot to keep walking, basic walking patterns are needed. One method to generate these patterns is to use an extrapolated center of mass (XcoM) concept and constant zero-moment point (ZMP) patterns. However, center of mass (CoM) patterns generated from such a method have discontinuous ZMP and CoM accelerations. For solving this problem, we propose a method in which continuous ZMP patterns can be simply generated from constant ones. In addition, experimental results of forward walking are presented. The results demonstrate that this pattern generation method can give a starting point for walking robots.**

I. INTRODUCTION

There is an increasing need in the world for robots that can work in disaster areas instead of human beings. To perform various tasks, robots have many requirements. Multijoint manipulators and end effectors suitable for different tasks are necessary hardware. Robot mobility is also crucial. Currently, movement can be divided into two groups: wheel- or caterpillar-based mobile platform groups and multilegged mechanism groups. Mobile platforms have the merits of movement velocity and posture stability but are limited when confronted with overcoming various obstacles, e.g., crossing a divided road, navigating stepping stones, or ascending and descending stairs. Multilegged mechanism systems have an advantage when it comes to these obstacles. However, to accomplish mobility in legged robots requires solving two kinds of problems: generating walking patterns and controlling posture stably. In this paper, we focus on a method to generate bipedal walking patterns.

Vukobratovic and Borovac [1] suggested a zero-moment point (ZMP) concept over 35 years ago. Since then many researchers have generated walking patterns for bipedal walking robots based on the ZMP because it enables bipedal robots to walk dynamically. The walking patterns should be generated such that the ZMP would be in a supporting polygon. Representative bipedal walking robots to which the ZMP has been applied include the Honda robots [2], especially ASIMO, HRP [3], and WABIAN [4] in Japan and HUBO [5] in Korea.

In this paper we introduce a method to generate bipedal walking patterns using the extrapolated center of mass (XcoM) based on the ZMP, apply its patterns to an experimental robot, and show some experimental results. Hof et al. [6] proposed an XcoM concept of the linear inverted pendulum model (LIPM). Hof [7] then demonstrated that walking control of the LIPM was simplified when the XcoM, instead of the CoM, was controlled. However, the generated ZMP patterns were discontinuous and a walking without double-support phase (DSP) was considered.

Takenaka et al. [8] analyzed the LIPM by decomposing its motion into a divergent component motion (DCM) and a convergent component motion. They showed that the deviation between the original ZMP patterns and the new ones was small by using the DCM when the walking patterns needed to change.

Pratt et al. [13] defined a capture point (CP), which is the same as the XcoM and DCM. This is a point on a ground to take a robot to a capture state, in which the kinetic energy of the robot is zero and can keep zero. They used a linear inverted pendulum plus flywheel model for stepping to the CP as well as using angular momentum.

Englsberger et al. [9] approached walking pattern generation using the CP tracking method, which is similar to the pattern generation method based on preview control [11]. For tracking the desired CP patterns, ZMP, which is a control input, was changed by the position error of the CP. Constant ZMP patterns were employed to get an analytic solution for the relation between the CP and the ZMP. Then, the desired reference DCM was modified from a constant DCM to a continuous DCM using a third polynomial interpolation [10].

The suggested method for bipedal walking pattern generation focuses on making continuous ZMP patterns from the constant ones to reach the desired XcoM position. Therefore, if the desired XcoM positions are used as footprints of a bipedal walking robot, the bipedal walking pattern can be generated simply.

In addition, the proposed walking pattern generation method is implemented on the experimental robot and its experimental results of forward walking are presented.

II. XCOM OF THE LIPM

The LIPM is widely used as a simple model of a bipedal walking robot and the following assumptions are applied to this model to simplify the ZMP equations:

- The total mass of the robot is a single point mass.
- The vertical position of the CoM is kept constant.

According to these assumptions the LIPM of the sagittal plane is presented in Fig. 1(a) and the ZMP equation of the model is

$$\ddot{x}_{cm} = \frac{g}{z_0}(x_{cm} - x_{zmp}), \tag{1}$$

where g, z_0, x_{cm}, and x_{zmp} are the acceleration of gravity, the constant height of the CoM, the CoM X position, and

[1]Sangsin Park and Jun-Ho Oh are with the Department of Mechanical Engineering, Korea Advanced Institute of Science and Technology (KAIST), Daejeon, 305-338, Korea {gakdagui, jhoh}@kaist.ac.kr

the X position of the ZMP, respectively. Since the LIPM

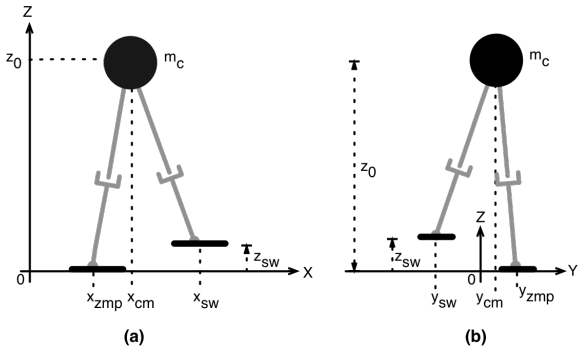

Fig. 1. LIPM of the (a) sagittal and (b) frontal planes

and the ZMP equation about the frontal plane are the same as those about the sagittal plane, these are not mentioned in this paper. Then, the XcoM position of the CoM is defined as

$$\xi_x = x_{cm} + \frac{1}{\omega_0}\dot{x}_{cm}, \tag{2}$$

where ξ_x is the X position of the XcoM and $\omega_0 = \sqrt{g/z_0}$. Since an eigenvalue of Eq. (2) is negative (i.e., Eq. (2) is stable), the CoM position follows any XcoM position. Consequently, we can consider the position of the XcoM instead of the CoM when generating walking patterns. By differentiating Eq. (2) with respect to time, we derive

$$\dot{\xi}_x = \dot{x}_{cm} + \frac{1}{\omega_0}\ddot{x}_{cm}. \tag{3}$$

Inserting Eq. (1) and (2) in Eq. (3) then gives

$$\dot{\xi}_x = \omega_0(\xi_x - x_{zmp}). \tag{4}$$

Because Eq. (4) is unstable, the position of the XcoM diverges exponentially for any inputs. Therefore, we need to bound the XcoM for appropriate walking patterns. The analytic solution of Eq. (4) is

$$\xi_x(t) = e^{\omega_0 t}\xi_{x,0} - \omega_0 \int_0^t e^{\omega_0(t-\tau)} x_{zmp}(\tau) d\tau. \tag{5}$$

From Eq. (5), we have that the XcoM position is changed by the convolution value of the ZMP. For convenience we let the second term of Eq. (5) be

$$h_x(t) = -\omega_0 \int_0^t e^{\omega_0(t-\tau)} x_{zmp}(\tau) d\tau. \tag{6}$$

We call this h value just after Eq. (6).

III. WALKING PATTERNS

For a bipedal robot to keep walking, some periodic walking footprints like those in Fig. 2 are needed.

The robot walks forward by using a walking pattern of alternating steps and keeping its CoM height constant. Its step length is L_{st} and the step time is t_{st}. This cyclic walking maintains constant step length and constant step time. So, we need to find the walking pattern of a single step, e.g., from

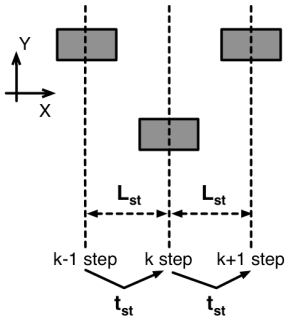

Fig. 2. Footprints of the LIPM

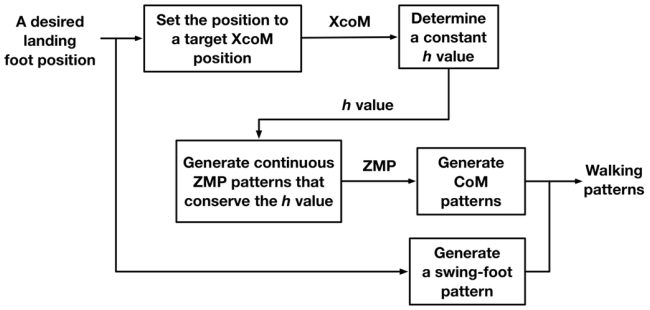

Fig. 3. Walking pattern generation procedure

the kth to the $(k+1)$th step. Our walking pattern is generated by using the following procedure (Fig. 3).

Once a desired landing foot position is determined, the position is set to a target XcoM position. Then a constant ZMP to reach the target XcoM position is calculated and a constant h value is determined. After this, continuous ZMP patterns with a DSP are generated by conserving the h value. Finally, the CoM patterns are generated through the newly generated ZMP patterns.

A. Constant ZMP

Because for a constant ZMP the convolution of Eq. (5) is simply calculated, let us consider the XcoM position for a single step in this case. From Eq. (5), we get

$$\xi_{x,k+1} = e^{\omega_0 t_{st}}\xi_{x,k} + x_{zmp,k}(1 - e^{\omega_0 t_{st}}), \tag{7}$$

where t_{st}, $\xi_{x,k}$, $\xi_{x,k+1}$, and $x_{zmp,k}$ are step period, a current position and next position of the CP, and a current ZMP, respectively. Eq. (7) can be rewritten as

$$x_{zmp,k} = \frac{\xi_{x,k+1} - e^{\omega_0 t_{st}}\xi_{x,k}}{1 - e^{\omega_0 t_{st}}}. \tag{8}$$

Eq. (8) is the required ZMP for a single step. By setting the kth foot position to $\xi_{x,k}$ and the $(k+1)$th foot position to $\xi_{x,k+1}$, we can get the constant ZMP. From Eq. (7), the constant h value is

$$h_{x,k} = x_{zmp,k}(1 - e^{\omega_0 t_{st}}). \tag{9}$$

B. Continuous ZMP pattern

Using a constant ZMP has the advantage of simplifying the calculation of the ZMP equation. However, as seen in

Fig. 4, a ZMP discontinuity appears between the p_k and the p_{k+1} (x-marked lines) at the switching legs. Because of this problem, the acceleration trajectory of the CoM also becomes discontinuous. To solve this problem, we assign the DSP time to the step time and suggest a new method to connect ZMP patterns continuously at that time. This method is composed of the following:

- A single ZMP pattern consists of linear functions at the DSP and a constant function at the single-support phase (SSP).
- At every single step a continuous ZMP pattern is generated to keep the h value of Eq. (9) the same.

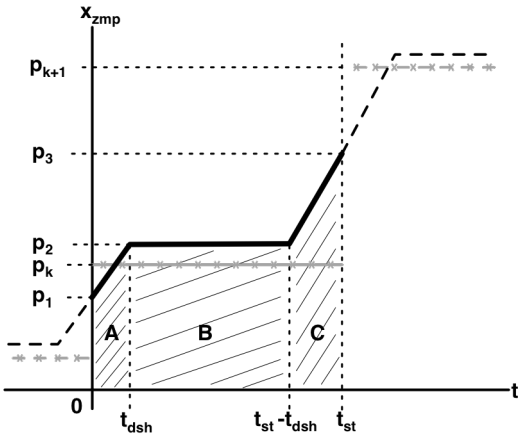

Fig. 4. Continuous ZMP pattern of the sagittal plane

Fig. 4 presents the continuous ZMP pattern generated by using this new method. Here, t_{st} and t_{dsh} are the walking period and the half time of the DSP, respectively. Moreover, p_1, p_k, p_2, and p_3 are the ZMP at the end of the previous step, a constant ZMP for the kth step, a constant ZMP at the SSP, and the ZMP at the end of the current step, respectively. When p_1, p_k, and p_3 are known, we can construct the ZMP pattern to determine p_2. The concept for generating the ZMP pattern is to find p_2 satisfying that the h value of the generated ZMP pattern is equivalent to Eq. (9), i.e.,

The h value of Eq. (9)
= (the h value of area A) + (the h value of area B)
+ (the h value of area) C.

Therefore,

$$
\begin{aligned}
& p_k(1-e^{\omega_0 t_{st}}) \\
&= e^{\omega_0(t_{st}-t_{dsh})}\{(p_2-p_1)\left(\frac{1-e^{\omega_0 t_{dsh}}}{\omega_0 t_{dsh}}+1\right) \\
&\quad +p_1(1-e^{\omega_0 t_{dsh}})\} \\
&\quad +e^{\omega_0 t_{dsh}}p_2(1-e^{\omega_0(t_{st}-2t_{dsh})}) \\
&\quad +(p_3-p_2)\left(\frac{1-e^{\omega_0 t_{dsh}}}{\omega_0 t_{dsh}}+1\right) \\
&\quad +p_2(1-e^{\omega_0 t_{dsh}}).
\end{aligned}
\tag{10}
$$

The left-hand side of Eq. (10) is the h value of the constant-ZMP case and the right-hand side is that of the continuous-ZMP case. Simplifying Eq. (10) with respect to p_2 gives

$$
\begin{aligned}
& \underbrace{\{e^{\omega_0 t_{st}}(e^{-\omega_0 t_{dsh}}-1)+e^{\omega_0 t_{dsh}}-1\}}_{c_1}\ p_2 \\
&= \omega_0 t_{dsh}\{e^{\omega_0 t_{st}}(p_1-p_k)+p_k-p_3\} \\
&\quad \underbrace{+e^{\omega_0 t_{st}}(e^{-\omega_0 t_{dsh}}-1)p_1+(e^{\omega_0 t_{dsh}}-1)p_3}_{c_2}. \\
& \therefore\ p_2=\frac{c_2}{c_1}.
\end{aligned}
\tag{11}
$$

During the SSP, the ZMP is kept constant as Eq. (11).

Because the ZMP pattern generated by this method gives an h value that is the same as that of the constant-ZMP pattern, the target XcoM position is no different from that in the constant-ZMP case. Fig. 5 shows six-step ZMP, XcoM, and CoM patterns generated by using this new method with a step period of 0.8 s, a DSP time of 0.1 s, and a step length of 0.2 m.

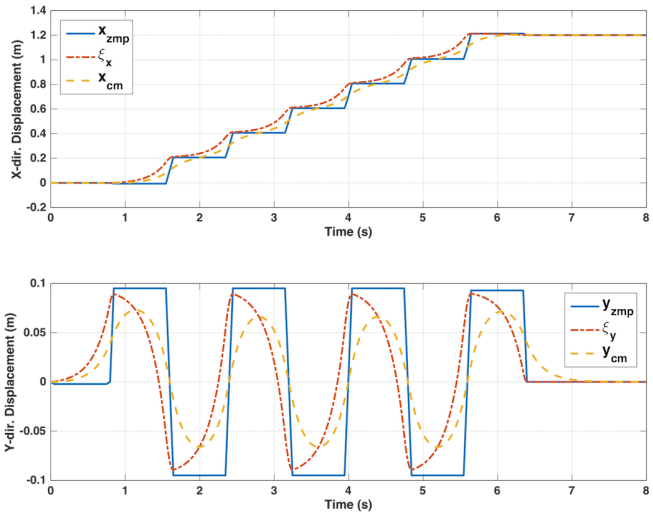

Fig. 5. CoM patterns in X and Y directions

IV. CONTROLLER

For the sake of implementing the suggested walking patterns, control loops (Fig. 6) are designed as follows.

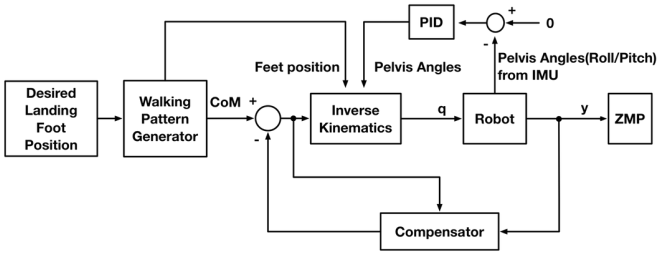

Fig. 6. Control loops

The control loops consist of a walking pattern generator to make CoM references, a compensator for ZMP control,

and proportional-integral-derivative controls for the upper body posture. The compensator, whose schematic is shown in Fig. 7, is composed of a closed-loop observer and full-state feedback [12].

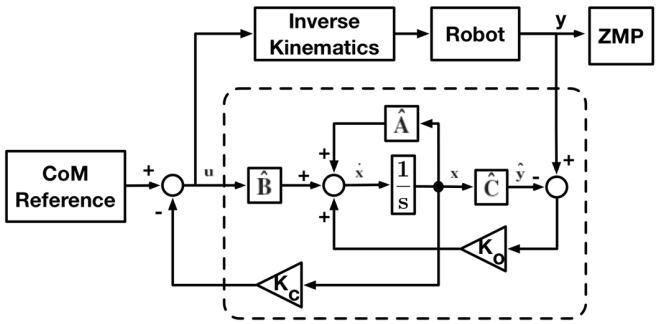

Fig. 7. Compensator

To determine the system model, step responses of the frontal and sagittal planes and a MATLAB® System Identification Toolbox™ are used. For the frontal plane, when an input CoM reference of step time = 3 s, DSP time = 0.1 s, and amplitude = 0.09 m is excited, the step response is presented in Fig. 8. As a result of using the System Identification Toolbox™, we find that a third-order system model is the minimum order for the best fit. Figs. 9 and 10 show a pole-zero map and a Bode plot of the third-order model, respectively. The resonance frequency of the model is 2.83 Hz and the model is a nonminimum phase system because of a zero in the right half-plane (RHP). A model in the sagittal plane is determined in the same way.

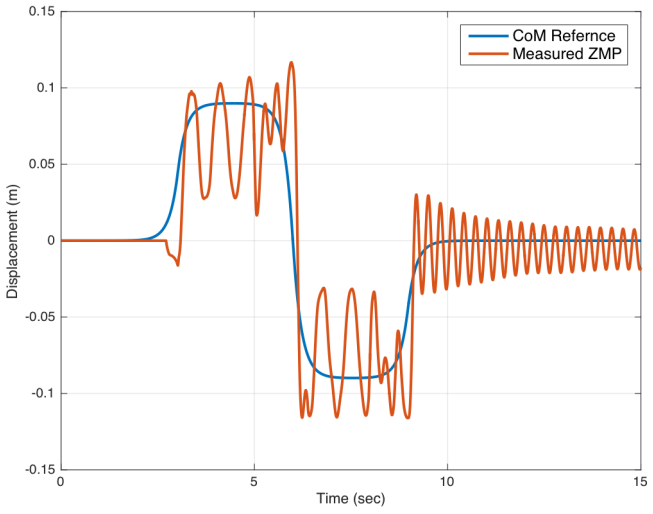

Fig. 8. A step response of the frontal plane

V. EXPERIMENTS

The experimental HUBO2 has 13 degrees of freedom (DOFs): six DOFs in each leg and 1 DOF for waist yaw. Fig. 11 shows the details. Digest specifications of the robot, which is except for motor powers, speed reducer ratios, link lengths, etc., and walking parameters are listed in Table I. The

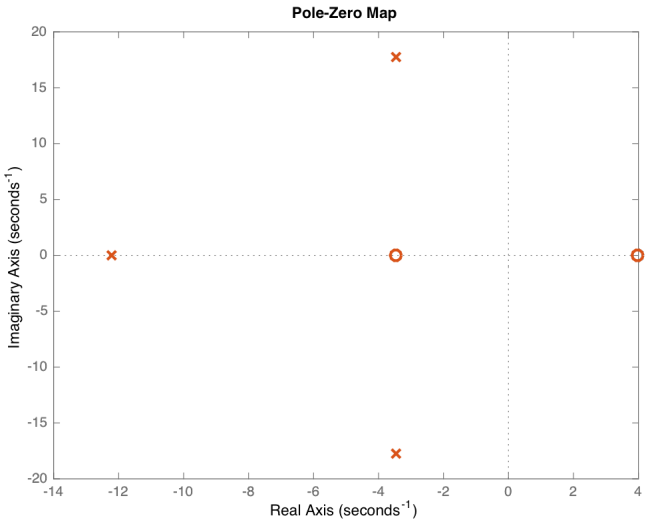

Fig. 9. A pole-zero map of the model

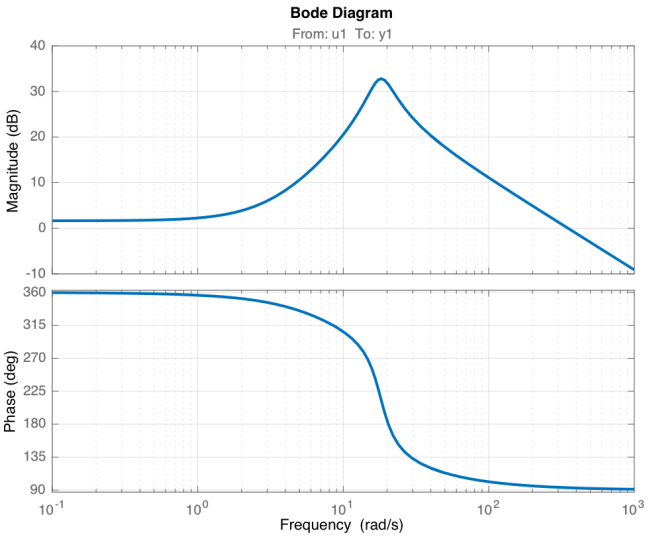

Fig. 10. A Bode plot of the model

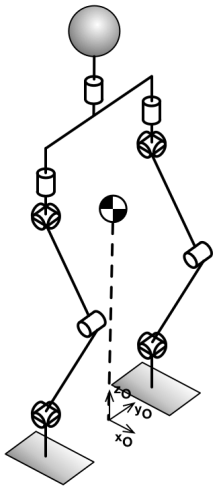

Fig. 11. Structure of the 13-DOF experimental HUBO2

proposed walking pattern generation method is implemented on the robot, which does not move its two arms.

In the following we present our experimental results for six-step forward walking with the parameters of Table I. Snapshots of the robot's movement are presented in Fig. 12. Fig. 13 shows the ZMP and CoM references, measurements of the X- and Y-direction ZMPs, and supporting polygons of the foot. The robot's stepping sequence starts from the first DSP (S_0, $S_{0'}$), then $S_0 \rightarrow (S_0,S_1) \rightarrow S_1 \rightarrow (S_1,S_2) \rightarrow \ldots \rightarrow S_6$, and finally it finishes walking at the last DSP (S_6, $S_{6'}$). Since the measured ZMPs in the X and Y directions are in each supporting area of foot, the robot walks forward stably without falling down. For greater detail, Figs. 14 and 15 show the reference and measured ZMPs of each direction separately. ZMP responses in both directions exhibit undershoot and, in the Y-direction case, just before the end of the SSP the foot touches the ground ahead of schedule. This phenomenon occurs when the robot's body leans inside during its SSP.

To reduce these unexpected ZMP errors, a inverse model and a body posture feedforward controllers need to be included.

TABLE I

DIGEST SPECIFICATIONS AND PARAMETERS OF THE EXPERIMENTAL HUBO2

Mass	39.2 kg
CoM height of a neutral position	0.45 m
Total degrees of freedom	13 (two legs and a waist)
No. of force/torque sensor axes	6
No. of inertial sensor axes	6
Step period	0.8 s
DSP time	0.1 s
Step length	0.2 m
Max. foot height of a swing leg	0.05 m
Walking speed	0.25 m/s (0.9 km/h)

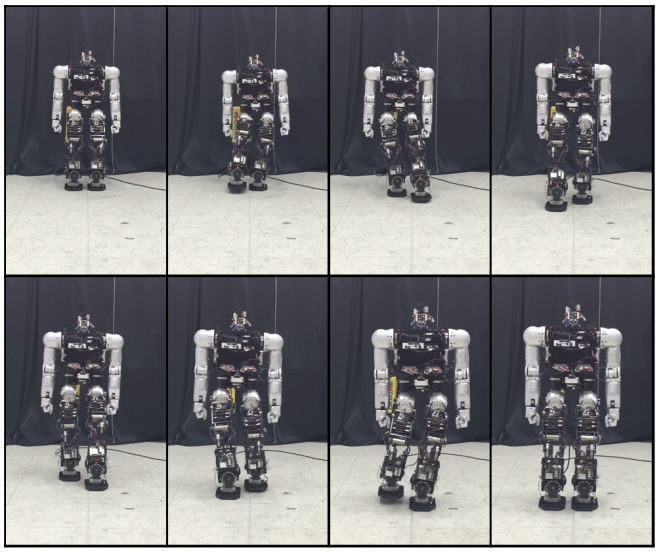

Fig. 12. Snapshots of six-step forward walking

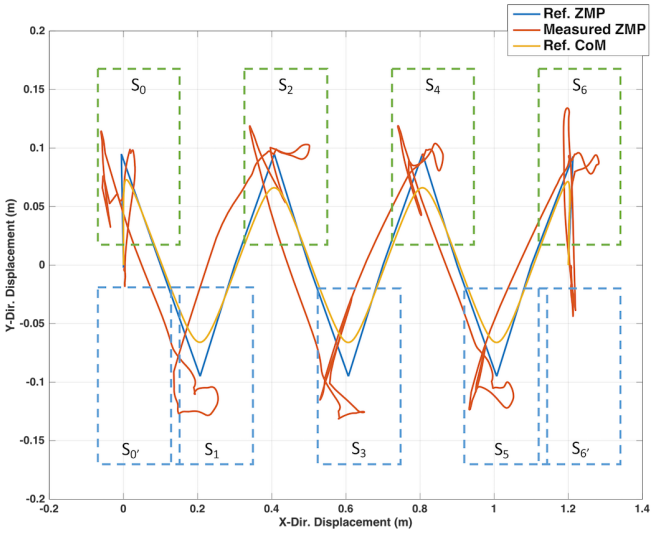

Fig. 13. Measured ZMPs in the X and Y directions

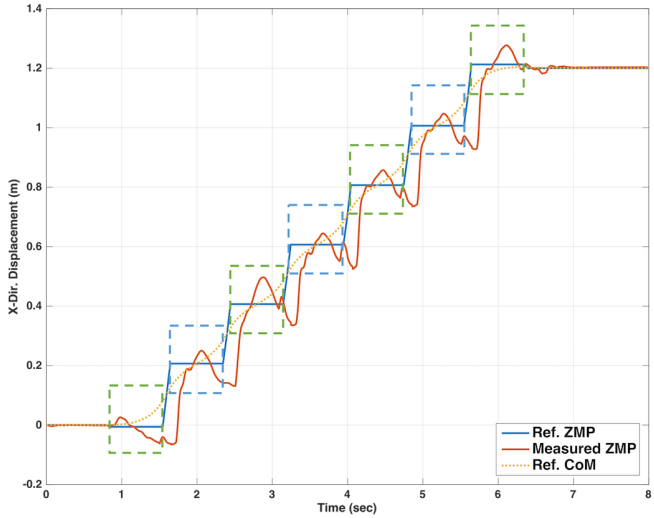

Fig. 14. Measured ZMP in the X direction

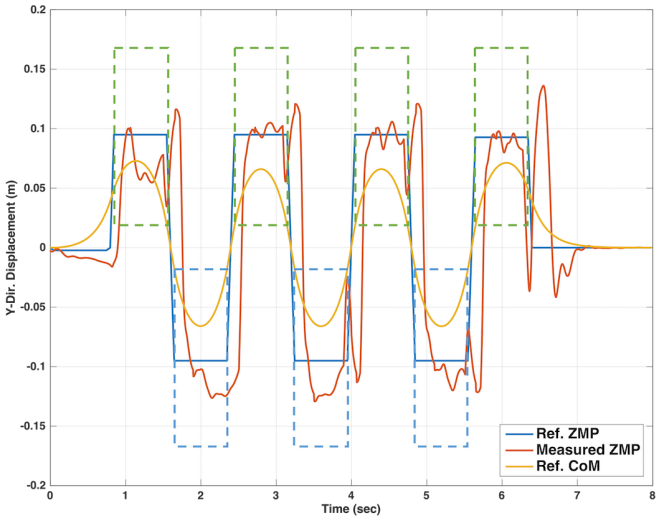

Fig. 15. Measured ZMP in the Y direction

VI. CONCLUSIONS

When a CoM pattern is generated by applying the XcoM concept and a constant ZMP, the CoM acceleration pattern is discontinuous. To resolve this problem, a new method was proposed to simply generate continuous ZMP patterns from the constant ones. When XcoM positions are determined by using landing foot positions, walking patterns could be simply constructed by using the suggested procedure. To realize these patterns with an experimental robot, a compensator was designed. As a result, the robot walked six steps forward periodically and stably, and experimental results were presented. Therefore this pattern generation method based on the XcoM is able to give a starting point for walking robots.

REFERENCES

[1] M. Vukobratovic and B. Borovac, "Zero-moment point - Thirty five years of its life," *Int. J. of Humanoid Robotics*, vol. 1, no. 1, 2004, pp. 157–173.

[2] K. Hirai, M. Hirose, Y. Haikawa, and T. Takenaka, "The development of Honda humanoid robot," *Proc. Int. Conf. Robot. Autom.*, vol. 2, 1998, pp. 1321–1326.

[3] S. Kajita, F. Kanehiro, K. Kaneko, K. Fujiwara, K. Yokoi, and H. Hirukawa, "A realtime pattern generator for biped walking," *Proc. Int. Conf. Robot. Autom.*, vol. 1, 2002, pp. 31–37.

[4] H.O. Lim, Y. Kaneshima, and A. Takanishi, "Online walking pattern generation for biped humanoid robot with trunk," *Proc. Int. Conf. Robot. Autom.*, vol. 3, 2002, pp. 3111–3116.

[5] I. W. Park, J. Y. Kim, and J. H. Oh, "Online walking pattern generation and its application to a biped humanoid robot - KHR-3 (HUBO)," *Adv. Robot.*, vol. 22, no. 2, 2008, pp. 159–190.

[6] A. L. Hof, M. Gazendam, and W. E. Sinke, "The condition for dynamic stability," *J. Biomech.*, vol. 38, no. 1, 2005, pp. 1–8.

[7] A. L. Hof, "The 'extrapolated center of mass' concept suggests a simple control of balance in walking," *Human Movement Sci*, vol. 27, no. 1, 2008, pp. 112–125.

[8] T. Takenaka, T. Matsumoto, and T. Yoshiike, "Real time motion generation and control for biped robot - 1st report: Walking gait pattern generation," *Proc. IEEE/RSJ Int. Conf. Intell. Robots Syst.*, 2009, pp. 1084–1091.

[9] J. Englsberger, C. Ott, M. A. Roa, A. Albu-Schaffer, and G. Hirzinger, "Bipedal walking control based on Capture Point dynamics," *Proc. IEEE/RSJ Int. Conf. Intell. Robots Syst.*, 2011, pp. 4420–4427.

[10] J. Englsberger, T. Koolen, S. Bertrand, J. Pratt, C. Ott, and A. Albu-Schffer, "Trajectory generation for continuous leg forces during double support and heel-to-toe shift based on divergent component of motion," *Proc. IEEE/RSJ Int. Conf. Intell. Robots Syst.*, 2014, pp. 4022–4029.

[11] S. Kajita, F. Kanehiro, K. Kaneko, K. Fujiwara, K. Harada, K. Yokoi, and H. Hirukawa, "Biped walking pattern generation by using preview control of zero-moment point," *Proc. IEEE Int. Conf. Robot. Autom.*, vol 2, 2003, pp. 1620–1626.

[12] G. F. Franklin, J. D. Powell, and A. Emami-Naeini, *Feedback Control of Dynamic Systems*, 5th ed, Pearson Prentice Hall, 2006, pp. 409–434.

[13] J. Pratt, J. Carff, S. Drakunov, and A. Goswami, "Capture point: A step toward humanoid push recovery," *IEEE-RAS Int. Conf. Humanoid Robots*, 2006, pp. 200–207.